STUDIA UBB CHEMIA, LVI, 4, 2011 (p. 89 - 97)

RAMAN AND SERS CHARACTERIZATION OF NORMAL PATHOLOGICAL SKIN

ALEXANDRA FĂLĂMAŞ[a,*], CRISTINA DEHELEAN[b], SIMONA CÎNTĂ PÎNZARU[a]

ABSTRACT. This study presents a Raman characterization of normal pathological mice skin both *in vivo* and *ex vivo*. Good correlation between the *in vivo* acquired spectra from the back of the mice specimens and the *ex vivo* formalin fixed skin samples was observed, although the *in vivo* spectra presented better resolved Raman bands. Additionally, using near-infrared laser excitation SERS spectra were acquired from the *ex vivo* skin samples immersed in Ag nanoparticles. The NIR-SERS spectra revealed main vibrational modes at 1573, 1327, 1227 and 227 cm^{-1} preponderantly characteristic to nucleic acids, which bring additional contribution to the chemical composition of the Raman investigated tissue.

Keywords: *Raman, SERS, mice skin, in vivo*

INTRODUCTION

Human and animal skin has been the subject of numerous spectroscopic investigations in the last years. Raman spectroscopy implies the detection of the inelastically scattered photons by the irradiated sample. Although the Raman signal is extremely weak, the main advantages of the technique rely on the fact that the sample requires minimal or no preparation and that the interface from water absorption is almost absent from the Raman spectra. The intensity of the active Raman bands is dependent on the concentration of the scattering species and independent on the sample thickness. Since the introduction of Raman spectroscopy for skin research [1], the technique has gained increasing popularity for both *in vivo* and *ex vivo* applications. Gniadecka et al. reported the in vitro Raman spectra of human skin, hair and nail [2], Caspers et al. investigated the properties of different skin layers using *in vivo* confocal Raman micro spectroscopy [3]. Additionally, the technique was used for the *in vivo* and *ex vivo* diagnosis of a variety of skin cancers [4-8].

[a] Babeş-Bolyai University, Faculty of Physics, 1 Kogălniceanu str., 400084 Cluj-Napoca, România
[b] Victor Babeş University of Medicine and Pharmacy, Faculty of Pharmacy, Eftimie Murgu Square 2, 300041 Timişoara, România
* *alexandra.falamas@ubbcluj.ro*

Regardless of the multitude applications of Raman spectroscopy, the technique has some disadvantages, as well. Firstly, of all the photons scattered by the sample only one in 10^6-10^8 represent the Raman signal. This inherently weak process can not be usually amplified by increasing the laser power because of the risk of damaging the sample. Another disadvantage of Raman spectroscopy is that fluorescence usually interferes with the Raman signal. Surface enhanced Raman signal (SERS) [9-11] can help overcome both problems, because of the amplification of the scattering efficiency per molecule and the adsorption process of the investigated sample to the metal surface which promotes fluorescence quenching. SERS at extremely high enhancement levels may transform Raman spectroscopy from a structural analytical tool to a sensitive single-molecule and nanoscale probe [12, 13] due to the favorable optical properties of the metallic nanostructures.

SERS has been lately used for a multitude of medical applications ranging from probing and imaging live cells [14], to developing SERS gene probes which can be used to detect DNA biotargets [15], to *ex vivo* diagnosing of normal and cancerous samples [16] and *in vivo* tumor targeting in live animals [17].

Other studies [18] have proved that the colloidal silver nanoparticles are able to penetrate the skin tissues and they were detected in the stratum corneum and the outermost surface of the epidermis. Our group has evidence before the possibility of acquiring SERS spectra from tissue samples [19, 20] and concluded that the Ag colloidal nanoparticles that can be incorporated into the interstitial space in the tissues allowed high quality SERS signal. Tissue differentiation based on the chemical composition changes would be suitable for surface enhanced Raman scattering since the ability to nanoparticles uptake has been proved. Different tissue structures have characteristic features in the SERS spectra and thus, SERS diagnosis of the samples is possible [16].

In this study we employed Raman and SERS spectroscopies for the characterization of mice skin, both *in vivo* and *ex vivo*. The aim of the research was to probe the molecular components from the skin tissues when investigating *in vivo* mice specimens versus *ex vivo* formalin fixed samples and to enhance the Raman signal of the autopsy tissue samples by employing the SERS effect.

RESULTS AND DISCUSSION

The *in vivo* Raman spectra acquired from the skin on the back of the healthy specimens (Fig.1 A) presented contributions from the main components of biological tissues: proteins, lipids, nucleic acids, carbohydrates and especially collagen. The main bands observed in the *in vivo* Raman spectra were assigned to proteins and lipids. These are the 1654 cm^{-1} (amide I band of proteins), 1445 cm^{-1} (CH_2 bending mode of lipids and proteins), 1003 cm^{-1} (phenylalanine) and 937 and 855 cm^{-1} (collagen). The Raman spectra acquired from the healthy mice skin were similar to those reported by other research groups obtained from

human and animal skin using near infrared and infrared excitation radiation for both *in vivo* or *ex vivo* measurements [2, 4, 21]. According to the current literature [2], the positions of the amide I and III bands at 1654 and 1269 cm^{-1}, as well as the presence of the well developed band at 937 cm^{-1} suggested a helical protein structure.

The 1200-1340 cm^{-1} spectral range presents mainly amide III bands of proteins and nucleic acids characteristic vibrational modes. These are the 1250 and 1269 cm^{-1} (amide III), the latter having the highest relative intensity in this region, the 1314 and 1338 cm^{-1} bands of guanine and CH_3CH_2 wagging of nucleic acids and collagen and adenine and guanine modes of DNA/RNA, respectively.

The 1030-1130 cm^{-1} spectral range presents useful information about the nature of the stratum corneum lipid bilayer packing [22]. C-C stretching modes of lipids are observed at 1127, 1087 and 1061 cm^{-1}. Additionally, these bands give information about the proteins as well, such as the 1127 cm^{-1} band assigned to C-N stretching modes of proteins and 1033 cm^{-1} band characteristic to C-H bending vibrations of phenylalanine of collagen [23].

Following the *in vivo* Raman measurements, autopsy samples were collected from the skin on the back of the rodents and further used for *ex vivo* Raman and SERS investigations. Fig.1 B) presents typical Raman spectra acquired from the formalin immersed skin sample. The spectra usually present the same fluorescent background as the *in vivo* Raman spectra and show the same main vibrations. Although, slight differences between the *in vivo* and the *ex vivo* Raman spectra can be observed. The 1200-1340 cm^{-1} spectral interval shows the same main components of tissues such as proteins, lipids and nucleic acids and the most intense peak is assigned to the amide III band of proteins as in the *in vivo* Raman spectra. In the 1030-1130 cm^{-1} range, the observed peaks are not as well resolved, although the Raman modes assigned to phenylalanine, the C-O stretching mode of carbohydrates, the C-C stretching vibrations of lipids as well as the C-N stretching mode of proteins can still be seen, usually slightly shifted when compared to the *in vivo* observed ones. Going towards lower wavenumbers, the main discrepancy is given by the absence of the proline band characteristic to collagen at 937 cm^{-1}. However, the main peak observed in this region is located at 919 cm^{-1} and is assigned to proline, as well [24]. On the other hand, the 853 cm^{-1} band is still present and shows the same band profile as seen in the *in vivo* spectra.

When passing from one spectrum to another the *ex vivo* Raman spectra showed basically the same profile and main bands, although some differences regarding the relative intensity of the bands or slight shiftings of the wavenumbers could be noticed. One explanation for this could be the inhomogenity of the skin tissues. Overall, the *ex vivo* Raman spectra matched well the *in vivo* ones and basing our assumptions on the above interpretations, we can conclude that the formalin fixation of tissues, did not affect significantly the acquisition of the spectral information.

Further aim of this research was to probe the Raman enhancement using Ag colloidal nanoparticles uptaken by the skin tissues along the formalin fixation. The autopsy skin samples collected from the mice specimens were immersed in 10% formalin solution mixed with colloidal silver.

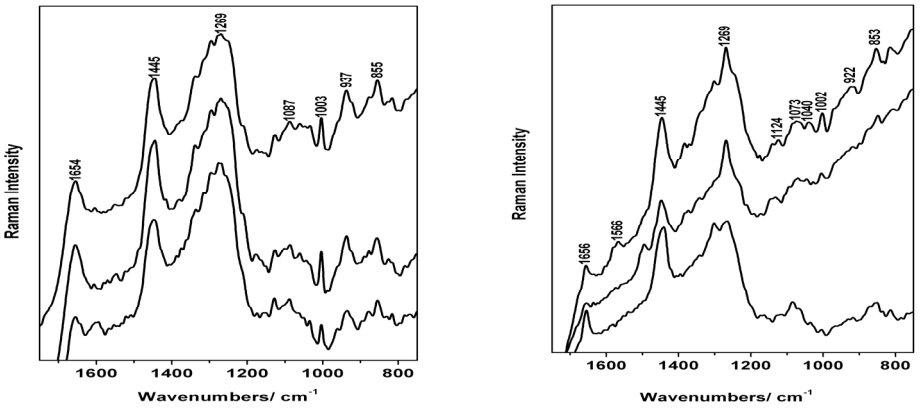

Figure 1. A) *In vivo* and B) *ex vivo* Raman spectra of healthy mice skin

Figure 2 presents several SERS spectra acquired from the healthy skin sample incubated with colloidal nanoparticles. The spectra were recorded using short acquisition times (3 to 5 seconds) and a strong tissue signaling with high specificity was obtained. The insertion in the figure shows the upper spectrum after background subtraction and zoom offset.

The most intense bands seen in the SERS spectra are located at 1573, 1443, 1327, 1227, 721, 652, 418 and 229 cm^{-1} (Figure 2). Other bands are observed as well, although having weaker relative intensity. The relative intensities in the SERS spectra are expected to differ significantly from the Raman ones, due to the adsorption behavior of certain molecules to the silver nanosurface. The SERS signal is expected from the molecular species located in the close vicinity of the uptaken nanoparticles, superimposed with the normal Raman scattering of the species from the laser focus area (< 1 μm). Due to the inherent inhomogenity of the tissue, the nanoparticles distribution is not uniform. Assuming that the Raman scattering effect is accompanied by the absorption, transmission as well as the elastic scattering, the rather low Raman efficiency would be much lower than the local SERS enhancement. Therefore, we assume the assignment of the recorded signal as being preponderantly SERS signal. According to the surface selection rules, the out of plane bending modes of a molecule adsorbed flat on the silver surface will be enhanced in the SERS spectra, while the in plane bending modes will be enhanced when the molecule is adsorbed perpendicular to the surface [25, 26].

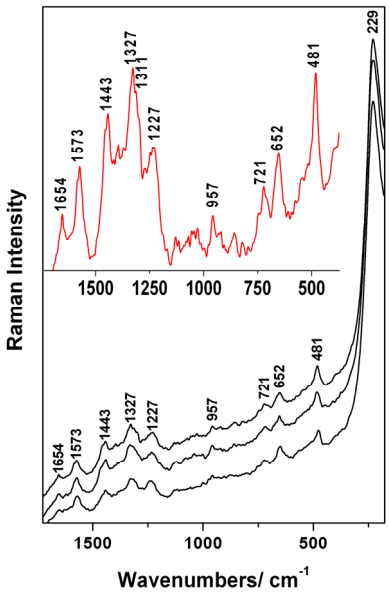

Figure 2. Typical SERS spectra acquired from the healthy mice skin tissue. The insertion shows a detailed SERS spectrum after background subtraction.

The main bands reported here were observed in our previous SERS studies as well, although at that time the main problem was the reproducibility of the spectra. It was surprising to observe in this study that the SERS spectra acquired from different points on the skin sample showed good reproducibility. Some of the vibrational modes observed here were reported by other research groups investigating the SERS effect in cells using gold or silver nanoparticles [27, 28]. Thus, the observed bands in our spectra can be assigned to the molecules or the molecular groups adsorbed to or in the close vicinity of the silver nanoparticles. The vibrational modes seen in the high wavenumber region of the spectra like the 1573 and 1443 cm^{-1} are assigned to nucleic acids constituents and proteins CH_2 and CH_3 bending vibrations, respectively. The 1380-1280 cm^{-1} spectral range exhibits an intense broad band centered at 1327 cm^{-1}. This Raman mode is assigned to phospholipids. This broad band contains other contributions as well, located at 1313 cm^{-1} assigned to nucleic acids and collagen and 1340 cm^{-1} assigned to bending mode of collagen and lipids [14, 29].

The same situation is seen for the 1280-1180 cm^{-1} spectral range which exhibits several contributions, as well. The most intense broad band observed here is centered at 1227 cm^{-1} and was assigned in the literature to the amide III band of proteins [30].

In the low wavenumber region of the spectra more nucleic acids bands can be observed, such as the 652 cm^{-1} band which may be assigned to a superposition of a tyrosine vibration and the guanine SERS fingerprint, or the 721 cm^{-1} assigned to adenine. The strongly enhanced sharp band seen at 229 cm^{-1} may indicate the formation of a metal-adsorbate bond, proving the interaction between the metal colloids and certain molecular species inside the skin tissue [31, 32].

Summarizing these findings, one could tentatively conclude that the silver nanoparticles penetrated the tissues along with the formalin in the fixation process.

CONCLUSIONS

This study presented a Raman and SERS characterization of healthy mice skin, serving as reference for further Raman skin diagnostic purpose. *In vivo* Raman investigations of the mice specimens were possible proving the efficiency of the technique for nondestructive and noninvasive studies. The interpretation of both *in vivo* and *ex vivo* Raman spectra revealed vibrational modes characteristic to proteins, lipids, nucleic acids and collagen. These findings prove that the formalin fixation of the autopsy collected skin samples did not affect significantly the acquisition of the Raman spectra.

By inoculating the samples with silver colloidal solution, it was possible to enhance the Raman signal characteristic to the skin tissues. The most intense vibrations were assigned to nucleic acids, although signal from proteins and lipids could be observed as well. These findings, as well as the intense band at 229 cm^{-1}, demonstrate the interaction between the metallic nanosurface and the adsorbate molecules in the tissues. The metal nanoparticles based SERS technique was applied here successfully as a sensitive, nondestructive spectroscopic method for the molecular structural probing in skin tissues.

EXPERIMENTAL PART

The Lee Meisel silver colloid was prepared through the standard method [33]. Briefly, 100 ml of a 1 mM $AgNO_3$ aqueous solution was heated to 93-100°C and then 2 ml of a 1% trisodium citrate solution was added. The mixture was kept in constant (previously achieved) temperature for about 1 hour and then was allowed to cool down to the room temperature. The resultant colloidal mixture was of dark grey color. Finally, the colloidal solution was centrifuged at 5500 rotations/min, for 5 min, resulting colloidal nanoparticles with extinction maximum at 420 nm and band half width of 50 nm. For the preparation of the solutions three distilled water was used.

Materials and methods

For this experiment BALB/c mice specimens were employed which were obtained from Charles River, Germany. The work protocol followed all NIAH-National Institute of Animal Health rules and the animals' regulations at the University of Medicine and Pharmacy Biobase, Timisoara, Romania. The animals were maintained during the experiment in standard conditions: 12h light-dark cycle, food and water ad libidum, temperature 24º C, humidity above 55%. At the time of the measurements, the mice specimens were 18 weeks old. After the *in vivo* Raman measurements, autopsy samples were collected from the skin on the back of the mice and immersed in formalin solution for further Raman investigations or formalin solution mixed with Lee Meisel silver colloid for the SERS measurements.

For the *in vivo* measurements, the mice were completely anesthesized with ketamine. The increased heart rate and breathing was monitored using the Raman microscope video-camera for defocussing reasons.

Instrumentation

For the Raman and SERS measurements a dispersive high performance micro-Raman spectrometer, Bruker Senterra with high spatial and spectral resolution was employed. The spectra were acquired using the 785 nm laser line and the exposure time for each spectrum was 3 to 5 s. The output laser power was set to 100 mW. The spectral resolution was 9 cm^{-1}.

ACKNOWLEDGMENTS

Financial support from the grant PN_II_IDEI 2284, 537/2008, ANCS, Romania is highly acknowledged. A. Falamas acknowledges support from the POSDRU/88/1.5/S/60185 project as well.

REFERENCES

1. A. Williams, H. Edwards, B. Barry, *Int. J. Pharm*., **1992**, *81*(2-3), 11
2. M. Gniadecka, P. Alshede Philipsen, S. Sigurdsson, S. Wessel, O. Faurskov Nielsen, D. HØjgaard Christensen, J. Hercogova, K. Rossen, H. Klem Thomsen, R. Gniadecki, L. Kai Hansen, H. Ch. Wulf, *J Invest Dermatol*., **2004**, *122*, 443
3. P. Caspers, G. Lucassen, G. Puppels, *Biophys. J.,* **2003**, *85*(1), 572
4. H. Wang, N. Huang, J. Zhao, H. Lui, M. Korbelika, H. Zeng, *J. Raman Spectrosc.,* **2011**, *42*(2), 160
5. Z. Huang, H. Zeng, I. Hamzavi, D. McLean, H. Lui, *Opt. Lett*, **2001**, *26*, 1782
6. N. Skrebova Eikje, K. Aizawa, T. Sota, Y. Ozaki, S. Arase, *The Open Medicinal Chemistry Journal*, **2008**, *2*, 38

7. M. Larraona-Puy, A. Ghita, A. Zoladek, W. Perkins, S. Varma, I.H. Leach, A.A. Koloydenko, H. Williams, I. Notingher, *J. Mol. Struct.,* **2010**, *993*(1-3), 57
8. S.B. Cartaxo, I.D. de Abranches Oliveira Santos, R. Bitar, A. Fernandes Oliveira, L. Masako Ferreira, H. Silva Martinho, A. Abrahão Martin, *Acta Cirúrgica Brasileira,* **2010**, *25*(4), 351
9. D.L. Jeanmarie, R.P. Van Duyne, *J. Electroanal. Chem.,* **1977**, *84*, 1
10. M.G. Albrecht, J.A. Creighton, J. *Electroanal. Chem.,* **1977**, *99*(15), 5215
11. M. Moskovits, *Reviews of Modern Physics*, **1987**, *57*(3), 783
12. K. Kneipp, H. Kneipp, J. Kneipp, *Acc. Chem. Res*., **2006**, *39*(7), 443
13. M.K. Gregas, F. Yan, J. Scaffidi, H.N. Wang, T. Vo-Dinh, *Nanomedicine: Nanotechnology, Biology and Medicine,* **2001**, *7*, 115
14. J. Kneipp, H. Kneipp, B. Witting, K. Kneipp, Nanomedicine: Nanotechnology, *Biology and Medicine*, **2010**, *6*, 214
15. T. Vo-Dinh, F. Yan, M.B. Wabuyele, *J. Raman Spectroscopy*, **2005**, *36*, 640
16. S. Cinta Pinzaru, L.M. Andronie, I. Domsa, O. Cozar, S. Astilean, *J. Raman Spectroscopy,* **2008**, *39*, 331
17. X. Qian, X.H. Peng, D.O. Ansari, Q.Y. Goen, G. Z. Chen, D.M. Shin, L. Yang, A.N. Young, M.D. Wang, S. Nie, *Nature Biotechnology*, **2008**, *26*(1), 83
18. F. Filon Laresea, F. D'Agostin, M. Crosera, G. Adami, N. Renzi, M. Bovenzi, G. Main, *Toxicology,* **2009**, *255*, 33
19. A. Falamas, S. Cinta Pinzaru, C.A. Dehelean, M.M. Venter, *Studia UBB Chemia*, **2010**, *2,* tom II, 273
20. A. Falamas, S. Cinta Pinzaru, C. Dehelean, Ch. Krafft, J. Popp, *Romanian Journal of Biophysics*, **2010**, *20*(1), 1
21. J. Zhao, H. Lui, D. McLean, H. Zeng, *Recent Advances in Biomedical Engineering*, **2010**, 455
22. B.W. Barry, H.G.M. Edwards, A.C. Williams, *J. Raman Spectroscopy*, **1992**, *23*, 641
23. S. Fendel, B. Schrader, *Fresenius' J Anal Chem*, **1998**, *360*(5), 609
24. Z. Movasaghi; S. Rehman; I.U. Rehman, *Applied Spectroscopy Reviews*, **2007**, *42*, 493
25. J.A. Creighton, "Spectroscopy of Surfaces - Advances in Spectroscopy", Wiley: New York, **1988**, vol. 16, p. 37 (Chapter 2)
26. X. Gao, J.P. Davies, M.J. Weaver, *J. Phys. Chem. A,* **1990**, *94*, 6858
27. K. Kneipp, A.S. Haka, H. Kneipp, K. Badizadegab, N. Yoshizawa, C. Boone, K.E. Shafer-Peltier, J.T. Motz, R.R. Dasari, M.S. Feld, *Appl. Spectr*., **2002**, *56*(2), 150
28. W.A. El-Saida, T.H. Kim, H. Kim, J.W. Choi, *Biosensors and Bioelectronics*, **2010**, *26*, 1486
29. O. Aydin, M. Kahraman, E. Kilic, M. Culha, *Appl. Spectr.,* **2009**, *63*(6), 662
30. H.W. Tang, X.B. Yang, J. Kirkham, D. Alastair Smith, *Appl. Spectr*., **2008**, *62*(10), 1060
31. A. Raj, K. Raju, H. Tresa Varghese, C.M. Granadeiro, H.I.S. Nogueirad, C.Y. Panicker, *J. Braz. Chem. Soc.,* **2009**, *20*(3), 549
32. T. Itoh, K. Hashimoto, V. Biju, M. Ishikawa, B.R. Wood, Y. Ozaki*, J. Phys. Chem. B,* **2006**, *110*, 9579
33. P.C. Lee, D. Meisel, *J. Phys. Chem.,* **1982**, *86*, 3391